



## Discovery and structure–activity relationships of a series of pyroglutamic acid amide antagonists of the P2X<sub>7</sub> receptor

Muna H. Abdi, Paul J. Beswick, Andy Billinton, Laura J. Chambers, Andrew Charlton, Sue D. Collins, Katharine L. Collis, David K. Dean, Elena Fonfria, Robert J. Gleave, Clarisse L. Lejeune, David G. Livermore, Stephen J. Medhurst, Anton D. Michel, Andrew P. Moses, Lee Page, Sadhana Patel, Shilina A. Roman, Stefan Senger, Brian Slingsby, Jon G. A. Steadman, Alexander J. Stevens, Daryl S. Walter\*

Neurosciences Centre of Excellence for Drug Discovery, GlaxoSmithKline, New Frontiers Science Park, Third Avenue, Harlow, Essex CM19 5AW, UK

### ARTICLE INFO

#### Article history:

Received 2 June 2010

Revised 6 July 2010

Accepted 8 July 2010

Available online 14 July 2010

#### Keywords:

P2X<sub>7</sub>

Antagonist

Pain

SAR

### ABSTRACT

A computational lead-hopping exercise identified compound **4** as a structurally distinct P2X<sub>7</sub> receptor antagonist. Structure–activity relationships (SAR) of a series of pyroglutamic acid amide analogues of **4** were investigated and compound **31** was identified as a potent P2X<sub>7</sub> antagonist with excellent in vivo activity in animal models of pain, and a profile suitable for progression to clinical studies.

© 2010 Elsevier Ltd. All rights reserved.

P2X<sub>7</sub>, an ATP-gated ion-channel,<sup>1–3</sup> controls the activation and release of pro-inflammatory cytokines such as interleukin-1 $\beta$  (IL-1 $\beta$ ).<sup>4</sup> Antagonists of the P2X<sub>7</sub> receptor can modulate such responses in P2X<sub>7</sub>-expressing cells in both the immune and central nervous systems,<sup>5</sup> suggesting a potential role for P2X<sub>7</sub> receptor antagonists in the treatment of a wide range of conditions. In particular, preclinical in vivo studies have directly implicated the P2X<sub>7</sub> receptor in pain states<sup>6</sup> and small molecule P2X<sub>7</sub> antagonists have been demonstrated to be efficacious in animal models of neuropathic pain.<sup>7–10</sup> Two compounds (AZD-9056 and CE-224535), have progressed to early proof-of-concept clinical trials in rheumatoid arthritis patients<sup>11,12</sup> and whilst both of these compounds have now been discontinued the question of whether a P2X<sub>7</sub> antagonist, with the appropriate physicochemical and pharmacokinetic profile, could be therapeutically efficacious in treating human pain states remains unanswered.

In two earlier publications<sup>13</sup> we described the optimization of a series of (1*H*-pyrazol-4-yl)acetamides, derived from hit compound **1** (Fig. 1) which had been identified via high-throughput screening. From this series, compound **2**, *N*-[(2,4-dichlorophenyl)methyl]-2-(3,5-dimethyl-1*H*-pyrazol-4-yl)acetamide, was selected for evaluation in in vivo models of pain and shown to be

a potent antihyperalgesic agent in both the rat acute complete Freund's adjuvant (CFA) model of inflammatory pain<sup>19</sup> and the knee joint model of chronic inflammatory pain.<sup>20</sup> However, compounds of this class were subsequently found to be prone to time-dependently inhibit the CYP3A4<sup>21</sup> isozyme and routes of metabolism studies indicated oxidation of the methyl substituents as the most likely cause.

Whilst this issue could be addressed (unpublished data) by replacing the methyl groups with alternative substituents (e.g.,

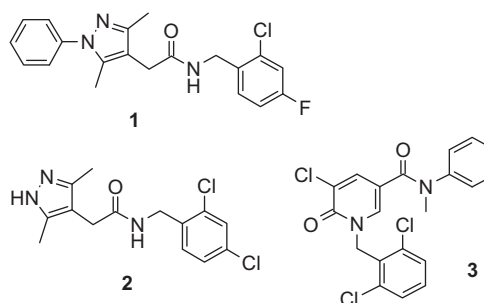


**Figure 1.** Compound **1**: human P2X<sub>7</sub> pIC<sub>50</sub><sup>14</sup> 7.4; rat P2X<sub>7</sub> pIC<sub>50</sub> 7.0; rat in vitro clearance<sup>15</sup> = 46 mL/min/g liver; c log *D*<sup>16</sup> at pH 7.4 = 3.4; *M*<sub>w</sub> = 372; LE = 0.39<sup>17</sup>; LLE<sup>18</sup> = 4.0; compound **2**: human P2X<sub>7</sub> pIC<sub>50</sub> 8.1; Rat P2X<sub>7</sub> pIC<sub>50</sub> 7.1; rat in vitro clearance 1.3 mL/min/g; c log *D* at pH 7.4 = 2.7; *M*<sub>w</sub> = 312; LE = 0.55; LLE = 5.4; compound **3**: human P2X<sub>7</sub> pIC<sub>50</sub> 6.9; rat P2X<sub>7</sub> pIC<sub>50</sub> 6.5; rat in vitro clearance >50 mL/min/g; c log *D* at pH 7.4 = 4.4; *M*<sub>w</sub> = 421; LE = 0.35; LLE = 2.5.

\* Corresponding author.

E-mail addresses: [daryl.s.walter@gsk.com](mailto:daryl.s.walter@gsk.com), [daryl@mail-web@yahoo.co.uk](mailto:daryl@mail-web@yahoo.co.uk) (D.S. Walter).

CF<sub>3</sub>) this usually resulted in a significant loss of potency. In order to address the potential developability risk presented by this observation we sought to identify alternative classes of P2X<sub>7</sub> antagonists which were free of this issue. Compound **3** (see Fig. 1) was also identified as a P2X<sub>7</sub> antagonist following our initial high-throughput screening of the GSK compound collection and, whilst this template was less attractive in general (higher molecular weight, lower ligand efficiency (LE)), it presented the opportunity to identify common pharmacophoric features that are shared by different P2X<sub>7</sub> antagonist chemotypes. In order to identify these common pharmacophoric features a simple overlay<sup>22</sup> of compounds **1** and **3** was performed. As can be seen in Figure 2 (circled) the resulting superposition of the two molecules indicated that the carbonyl oxygens of the two (acyclic) amide groups as well as the pyrazole nitrogen in **1** and the oxygen atom of the carbonyl in the pyridone ring of **3**, respectively, can interact with the same putative hydrogen-bond donor feature of the P2X<sub>7</sub> receptor in each case.

This observation led us to adopt the hypothesis that two suitably positioned hydrogen-bond donor features are required (or at least beneficial) when trying to achieve activity at the P2X<sub>7</sub> receptor in a low molecular weight template. Since only limited SAR was available (particularly around compound **3**) and we felt that we did not have sufficient information to build a pharmacophore that would be fit for virtual screening we decided to use fingerprint-based similarity searching in order to identify additional chemotypes of interest.<sup>23</sup> After applying property filters (e.g., hydrogen-bond acceptor count  $\geq 2$ , based on the overlay shown in Fig. 2) hits of interest were selected by stepping through the framework clusters and visually inspecting the members of the individual clusters.<sup>24</sup> A preference was given to molecules where the bond count between the two hydrogen-bond acceptor atoms was similar to that found in the query molecules (i.e., 5 in **1** and 6 in **3**).

The most promising hit with a ligand efficiency = 0.43<sup>17</sup> was pyroglutamic amide **4** (see Fig. 3), one of only nine compounds selected for screening, and ranked 595th amongst the 2000 top-ranked hits from the 3-point pharmacophoric fingerprint similarity search.<sup>26</sup> Whilst the human potency was good, the potency at the rat receptor was lower than preferred, but the low molecular

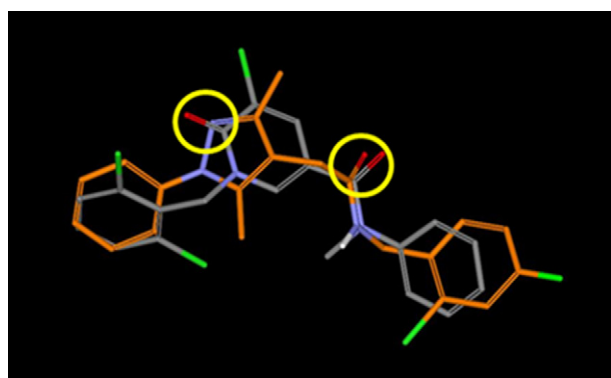


Figure 2. Overlay of compounds **1** (in orange) and **3**.

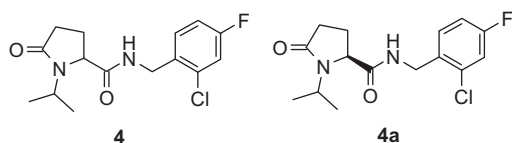
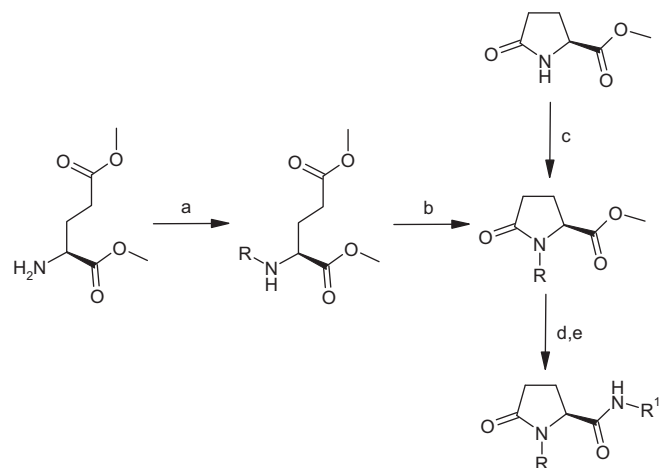


Figure 3. Compound **4**: human P2X<sub>7</sub> pIC<sub>50</sub> 6.5; rat P2X<sub>7</sub> pIC<sub>50</sub> <5; c log D at pH 7.4 = 2.6; M<sub>w</sub> = 312; LE = 0.43<sup>17</sup>; LLE = 3.9.<sup>18</sup> Compound **4a**: human P2X<sub>7</sub> pIC<sub>50</sub> 7.0; rat P2X<sub>7</sub> pIC<sub>50</sub> 5.8; rat in vivo clearance 31 mL/min/kg.



Scheme 1. Synthesis of pyroglutamic acid amide analogues. Reagents and conditions: (a) aldehyde or ketone, AcOH, NaBH<sub>4</sub>, MeOH, 0 °C, ca. 1 h; (b) toluene, reflux, Dean–Stark, ca. 16 h; (c) NaHMDS, alkyl halide, THF, –78 °C to room temperature, ca. 1 h; or aryl bromide, Pd<sub>2</sub>(dba)<sub>3</sub>, Cs<sub>2</sub>CO<sub>3</sub>, Xantphos™, toluene, reflux, ca. 18 h (d) 2M NaOH (aq), MeOH, 0 °C to room temperature, ca. 4 h (e) R<sup>1</sup>NH<sub>2</sub>, EDAC, HOBT, DCM/DMF (~3:1), rt, ca. 16 h.

weight and good ligand efficiency of **4** were particularly appealing. Synthesis of the (*S*)-enantiomer of **4** (i.e., **4a**) confirmed the activity of the initial sample and we resolved to prepare additional analogues to profile this template more thoroughly.

Analogues were, in the first instance, prepared using one of two methods as shown in Scheme 1.<sup>27</sup>

Reductive alkylation of the dimethyl ester of glutamic acid followed by thermal cyclisation gave the required *N*-substituted methyl pyroglutamates. Alternatively these key intermediates could be accessed by alkylation of methyl pyroglutamate with an alkyl halide or arylation using Buchwald coupling conditions. Subsequent saponification and amide coupling then provided the *N*-substituted pyroglutamic acid amides in good overall yields.

Using the above methods we first prepared a number of analogues which retained the 2-Cl, 4-F-benzamide group and explored the structure–activity relationships (SAR) around the *N*-alkyl substituent in the five-membered ring (Table 1). Removing the isopropyl group in **4a** resulted in a complete loss of activity (**5**) whereas replacement by methyl, ethyl and propyl gave

Table 1  
Structure–activity data for pyroglutamic acid amide analogues of compound **4**

Compd	R	Human P2X <sub>7</sub> pIC <sub>50</sub> <sup>a</sup>	Rat CLi <sup>b</sup> (mL/min/g) liver	Ligand efficiency <sup>17</sup>
<b>5</b>	H	<6	–	–
<b>6</b>	Me	7.0	–	0.50
<b>7</b>	Et	7.5	<0.5	0.52
<b>8</b>	<i>n</i> -Pr	6.8	–	0.45
<b>9</b>	2-Me-propyl	6.4	–	0.40
<b>10</b>	Benzyl	<6	–	–
<b>11</b>	Cyclobutyl	7.6	2.3	0.47
<b>12</b>	Cyclopentyl	6.3	–	0.38
<b>13</b>	Phenyl	6.1	–	0.35

<sup>a</sup> Data generated using an ethidium bromide release assay (Ref. 14), reporting an average value of *n* > 3.

<sup>b</sup> Microsomal clearance method described in Ref. 15.

analogues (**6**, **7** and **8**) with similar or slightly better potency in the case of the ethyl group.

Larger groups than this tended to have lower activity (e.g., **9**) and substitution with benzyl (**10**) was particularly detrimental to activity. Small cycloalkyl groups such as cyclobutyl (**11**) were as active as the ethyl analogue and this activity again dropped off as the ring size was increased (e.g., **12**) or if aromatic groups (e.g., **13**) were introduced.

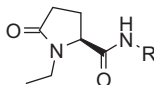
Encouragingly, in the cases where data was generated, compounds in this series demonstrated low levels of in vitro clearance in rat microsomes (see Table 1) and showed very little propensity to inhibit any of the CYP<sub>450</sub> enzyme isoforms tested (i.e., 1A2, 2C9, 2C19, 2D6, and 3A4—data not shown). There was also no evidence of time-dependent inhibition of the CYP<sub>450</sub> 3A4 enzyme thus addressing the concerns with the pyrazole series exemplified by compound **2**.<sup>13</sup>

To explore the SAR of the right-hand benzamide we chose to use the *N*-ethyl-substituted analogue **7** (the most ligand efficient analogue prepared up to this point) as the basis for comparison of different amide substituents. A subset of the compounds prepared are listed in Table 2. The cyclohexylmethyl **14** and simple benzyl **15** amides were essentially inactive. The adamantyl methyl group **16** (reported<sup>9</sup> to be a preferred substituent in a number of other literature examples of P2X<sub>7</sub> antagonists) was more active but not as good as the original 2-Cl, 4-*F*-benzylamide. Lipophilic substitution of the benzyl ring resulted in compounds with modest activity, regardless of the position substituted (see Cl-substituted analogues **17**, **18** and **19**). A CF<sub>3</sub> group in the 3-position **20** was, however, more active than the 2-substituted analogue **21**. More polar substituents (e.g., 2-OMe, **22**) of the benzyl ring were not well tolerated.

Significant improvements in potency and ligand efficiency relative to the initial hit compound **4** were observed with disubstituted benzylic amides in which both of the 2- and 3- or 4-positions were substituted with a lipophilic group. The 2,3- and 2,4-dichlorobenzylamides, **23** and **24**, were considerably more potent than the monosubstituted analogues and the 2-Cl, 3-CF<sub>3</sub>-benzylamide **25**, in particular, was the most potent analogue prepared thus far.

Analogues incorporating modifications to the pyrrolidinone ring are listed in Table 3. When the ring-carbonyl oxygen in **7** was removed, to give the corresponding proline derivative **26**, most of the activity was lost. Whilst this is not conclusive proof of an H-bonding interaction as postulated in the initial hypothesis used

**Table 2**  
Structure–activity data for a range of *N*-ethyl pyroglutamides



Compd	Ligand efficiency <sup>17</sup>	Human P2X <sub>7</sub> pIC <sub>50</sub> <sup>a</sup>	R
<b>14</b>	Cyclohexylmethyl	<6	—
<b>15</b>	Benzyl	<6	—
<b>16</b>	Tricyclo[3.3.1.1 <sup>3,7</sup> ]dec-1-ylmethyl	7.1	0.44
<b>17</b>	2-Cl-phenylmethyl	6.2	0.45
<b>18</b>	3-Cl-phenylmethyl	6.0	0.44
<b>19</b>	4-Cl-phenylmethyl	6.2	0.45
<b>20</b>	3-CF <sub>3</sub> -phenylmethyl	7.0	0.43
<b>21</b>	2-CF <sub>3</sub> -phenylmethyl	6.2	0.38
<b>22</b>	2-OMe-phenylmethyl	<6	—
<b>23</b>	2,3-DiCl-phenylmethyl	7.9	0.54
<b>24</b>	2,4-DiCl-phenylmethyl	8.2	0.56
<b>25</b>	2-Cl-3-CF <sub>3</sub> -phenylmethyl	8.8	0.53

<sup>a</sup> Data generated using an ethidium bromide release assay (Ref. 14), reporting an average value of *n* > 3.

**Table 3**  
Structure–activity data for analogues of compound **4**

Compd	R	Human P2X <sub>7</sub> pIC <sub>50</sub> <sup>a</sup>
<b>7</b>		7.5
<b>26</b>		<6
<b>27</b>		7.0
<b>28</b>		<6
<b>29</b>		6.8
<b>30</b>		7.5

<sup>a</sup> Data generated using an ethidium bromide release assay (Ref. 14), reporting an average value of *n* > 3.

to identify this series, acylating the ring nitrogen returned most of the activity (see **27**), possibly suggesting an H-bond with the carbonyl via an interaction along a slightly different vector. The amide NH also appeared to be important for receptor binding as methylation led to inactive compounds (e.g., **28** cf. the analogous NH amide, pIC<sub>50</sub> = 7.9). Inverting the stereochemistry of compound **7** led to only a modest reduction in activity (**29**), whilst expanding the five-membered ring to a six-membered ring (e.g., **30**) was well tolerated resulting in equipotent analogues.

Combination of the findings summarized above informed the preparation of additional analogues and compound **31** (see Fig. 4) subsequently emerged as a clear frontrunner with the best overall property profile. This compound incorporates the favoured 2-Cl-3-CF<sub>3</sub>-benzylamide moiety and the methyl substituent on the N atom of the lactam. Whilst the latter was not generally the most potent substituent it tended to provide compounds with the best balance of potency and pharmacokinetic properties.

Compound **31** had excellent potency at the human receptor but considerably lower affinity for the rat receptor (~100-fold lower); low clearance in rat and human liver microsomes; no appreciable inhibition of the CYP<sub>450</sub> enzyme isoforms tested (as above) up to concentrations of 100 μM; and no time-dependent inhibition of any of these isoforms.<sup>21</sup>

Following intravenous administration (1 mg/kg) to rats, compound **31** (see Table 4) had low blood clearance (9 mL/min/kg); a

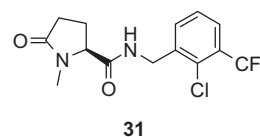


**Figure 4.** Human P2X<sub>7</sub> pIC<sub>50</sub> 8.5; rat P2X<sub>7</sub> pIC<sub>50</sub> 6.5; rat and human in vitro clearance <0.5 mL/min/g; CYP<sub>450</sub> inhibition pIC<sub>50</sub> >100 μM at all isoforms tested; log *D* at pH 7.4 = 1.9; *M*<sub>w</sub> = 334; LE = 0.53<sup>17</sup>; LLE = 6.2.<sup>18</sup>

**Table 4**  
Summary of the pharmacokinetic profile ( $n = 3$ ) of compound **31**

Route of administration	Dose	Property	Measured value
IV <sup>a</sup>	1 mg/kg	Clb (mL/min/kg)	9
		$T_{1/2}$ (h)	1.5
		$VD_{ss}$ (L/kg)	1.1
		$T_{max}$ (h)	1.0
PO <sup>b</sup>	3 mg/kg	$C_{max}$ ( $\mu$ M)	2.45
		AUC/dose (min kg/L)	73
		$F_{po}$	65%

<sup>a</sup> Compound **31** was dissolved in 0.9% (w/v) saline containing 10% (w/v) hydroxypropyl- $\beta$ -cyclodextrins (HPB) and 2% (v/v) DMSO at a target concentration of 0.2 mg/mL. It was administered as a 1 h intravenous infusion to achieve a target dose of 1 mg/kg.

<sup>b</sup> Compound **31** was dissolved in 1% (w/v) methylcellulose in water at a concentration of 0.6 mg/mL and dosed by oral gavage at a target dose of 3 mg/kg.

steady-state volume of distribution of 1.1 L/kg; and a half-life of 1.5 h. Compound **31** was rapidly absorbed ( $C_{max}$  achieved within 1 h) following a 3 mg/kg oral dose and had a bioavailability of 65%.

Compound **31** is a selective antagonist of the P2X<sub>7</sub> receptor, showing no appreciable off-target activities (>90 targets, both in-house and CEREP<sup>28</sup> selectivity panels). Whilst the rat receptor affinity of **31** is relatively modest we were confident that the selectivity for the P2X<sub>7</sub> receptor along with the high exposures obtained on oral dosing in rats, excellent solubility (0.97 mg/mL in FeSSIF<sup>29</sup>), and low protein binding (60% in rat plasma) would allow us to reliably evaluate the efficacy of this compound in animal models of pain.<sup>30</sup>

Indeed, compound **31** produced (Fig. 5) a highly significant and dose-related reversal of FCA-induced hypersensitivity in the knee joint model of chronic inflammatory pain.<sup>20</sup> Twice daily doses of 20 and 50 mg/kg produced a maximal reversal of hypersensitivity which was not statistically different to that obtained with the standard, celecoxib. Average blood and brain concentrations of **31** at 50 mg/kg, 1.5 h post-dose, were 26.7 and 12.9  $\mu$ M, respectively.

The efficacy of **31** in the rat chronic constriction injury (CCI)<sup>31</sup> model of nerve injury-induced allodynia was also explored (Fig. 6). In this model compound **31** (20 mg/kg, po, b.i.d. for 8 days) significantly reversed mechanical allodynia 1 h post dose on day 1 and this effect was maintained for the duration of the dosing period. The efficacy of **31** was not statistically different to that obtained with the standard gabapentin (30 mg/kg, po, b.i.d. for 8 days) at any time during the dosing period. Blood and brain concentrations taken after testing on the final day of dosing were 5.91 and 3.36  $\mu$ M, respectively (i.e., efficacy confirmed at free exposures higher than the rat  $pIC_{50}$  in the periphery and CNS in both in vivo studies).

In summary, we developed a simple P2X<sub>7</sub> pharmacophore and used this in combination with fingerprint-based similarity searching to identify a new series of drug-like P2X<sub>7</sub> antagonists with good

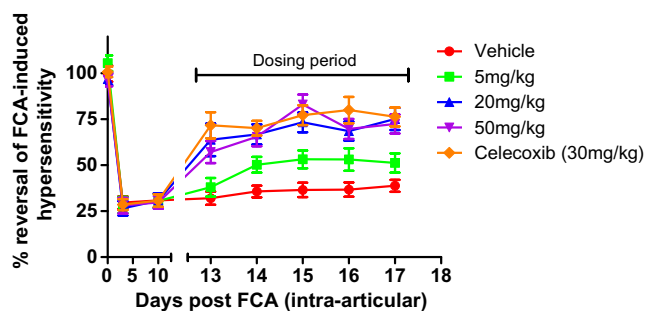


**Figure 5.** Effect of oral dose of **31** in the chronic joint pain model in the rat at oral doses of 5, 20 and 50 mg/kg b.i.d. for 5 days. The effect of 5 days oral dosing of 30 mg/kg b.i.d. celecoxib is included for comparison.

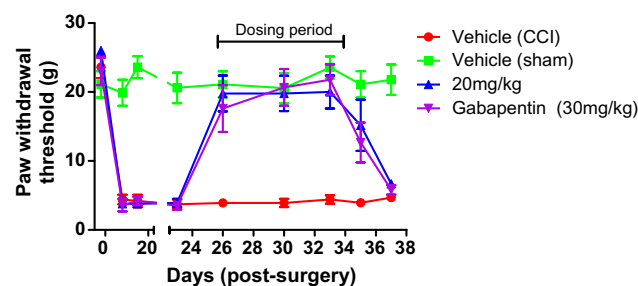


**Figure 6.** Effect of oral dose of **31** in the chronic constriction injury model in the rat at oral doses of 20 mg/kg b.i.d. for 8 days. The effect of 8 days oral dosing of 30 mg/kg b.i.d. gabapentin is included for comparison.

in vitro potency, selectivity, and pharmacokinetic properties, and which do not time-dependently inhibit the CYP<sub>450</sub> 3A4 enzyme. Compound **31** was shown to have good efficacy in both the chronic joint pain model of inflammatory pain and the CCI model of neuropathic pain. Compound **31** was thus identified as having clear potential as a therapeutic agent for the treatment of pain and addressed the developability concerns highlighted earlier for compounds such as **2**. Compound **31** was subsequently selected for progression into early phase clinical studies. Details of these studies will be disclosed in a future publication.

## References and notes

- Collo, G.; Neidhart, S.; Kawashima, E.; Kosco-Vibois, M.; North, R. A.; Buell, G. *Neuropharmacology* **1997**, *36*, 1277.
- DiVirgilio, F.; Vishwanath, V.; Ferrari, D. In *Handbook of Experimental Pharmacology*; Abbraccio, M. P., Williams, M., Eds.; Springer, 2001; Vol. 151, pp 355–373.
- Buisman, H. P.; Steinberg, T. H.; Fischbar, J.; Silverstein, S. C.; Vogelzang, S. A.; Ince, C.; Ypey, D. L.; Leijh, P. C. *Proc. Natl. Acad. Sci. U.S.A.* **1988**, *85*, 7988.
- Ferrari, D.; Pizzirani, C.; Adinolfi, E.; Lemoli, R. M.; Curti, A.; Idzko, M.; Panther, E.; Di Virgilio, F. *J. Immunol.* **2006**, *176*, 3877.
- Fields, D.; Burnstock, G. *Nat. Rev. Neurosci.* **2006**, *7*, 423.
- Chessel, I. P.; Hatcher, J. P.; Bountra, C.; Michel, A. D.; Hughes, J. P.; Green, P.; Egerton, J.; Murfin, M.; Richardson, J.; Peck, W. L.; Grahames, C. B. A.; Casula, M. A.; Yiangou, Y.; Birch, R.; Anand, P.; Buell, G. *N. Pain* **2005**, *114*, 386.
- Honore, P. M.; Donnelly-Roberts, D.; Namovic, M.; Hsieh, G.; Zhu, C.; Mikusa, J.; Hernandez, G.; Zhong, C.; Gauvin, D. M.; Chandran, P.; Harris, R.; Medrano, A. P.; Carroll, W.; Marsh, K.; Sullivan, J. P.; Faltynek, C. R.; Jarvis, M. F. *J. Pharmacol. Exp. Ther.* **2006**, *319*, 1376.
- Broom, D. C.; Matson, D. J.; Bradshaw, E.; Buck, M. E.; Meade, R.; Coombs, S.; Matchett, M.; Ford, K. K.; Yu, W.; Yuan, J.; Sun, S. H.; Ochoa, R.; Krause, J. E.; Wustrow, D. J.; Cortright, D. N. *J. Pharmacol. Exp. Ther.* **2008**, *327*, 620.
- Perez-Medrano, A.; Donnelly-Roberts, D. L.; Honore, P.; Hsieh, G. C.; Namovic, M. T.; Peddi, S.; Shuai, Q.; Wang, Y.; Faltynek, C. R.; Jarvis, M. F.; Carroll, W. A. *J. Med. Chem.* **2009**, *52*, 3366.
- Nelson, D. W.; Gregg, R. J.; Kort, M. E.; Perez-Medrano, A.; Voight, E. A.; Wang, Y.; Grayson, G.; Namovic, M. T.; Donnelly-Roberts, D. L.; Niforatos, W.; Honore, P.; Jarvis, M. F.; Faltynek, C. R.; Carroll, W. A. *J. Med. Chem.* **2006**, *49*, 3659.
- McInnes, I. B.; Snell, N. J.; Perrett, J. H.; Parmar, H.; Wang, M. M.; Astbury, C. *Arthritis Rheum.* [71st Annu Sci Meet Am Coll Rheumatol (Nov 6–11, Boston) 2007] **2007**, *56*, Abst 2085.
- ClinicalTrials.gov Identifier: NCT00628095.
- (a) Chambers, L. J.; Stevens, A. J.; Moses, A. P.; Michel, A. D.; Slingsby, B.; Walter, D. S.; Davies, D. J.; Livermore, D. J.; Fonfria, E.; Demont, E. H.; Vimal, M.; Theobald, P. J.; Beswick, P. J.; Gleave, R. J.; Roman, S. A.; Senger, S.; Roomans, S. *Bioorg. Med. Chem. Lett.* **2010**, *20*, 3161; (b) Beswick, P. J.; Billinton, A.; Chambers, L. J.; Dean, D. K.; Fonfria, E.; Gleave, R. J.; Medhurst, S. J.; Michel, A. D.; Moses, A. P.; Patel, S.; Roman, S. A.; Roomans, S.; Senger, S.; Stevens, A. J.; Walter, D. S. *Bioorg. Med. Chem. Lett.* **2010**, *20*, 4653.
- Potencies are measured using a competition experiment using the natural ligand ATP. ATP activation leads to formation of a large opening in the cell wall and accumulation of ethidium bromide dye within the cell, levels of which are measured using fluorescence. All test compounds had  $I_{max}$  values of 100%. Full details of the assay protocol can be found in patent application WO 2007 141267 A1.
- Clarke, S. E.; Jeffrey, P. *Xenobiotica* **2001**, *31*, 591.
- Calculated log  $D$  values were obtained using ACD Labs software v8.0.
- Abad-Zapatero, C. *Expert Opin. Drug Discovery* **2007**, *2*, 469.
- (a) Leeson, P. D.; Springthorpe, B. *Nat. Rev. Drug Disc.* **2007**, *6*, 881; The same concept was independently proposed by researchers at Pfizer and termed lipE. (b) Ryckmans, T.; Edwards, M. P.; Horne, V. A.; Monica Correia, A.; Owen, D. R.;

- Thompson, L. R.; Tran, I.; Tutt, M. F.; Young, T. *Bioorg. Med. Chem. Lett.* **2009**, *15*, 4406.
19. Iadarola, M. J.; Douglass, J.; Civelli, O.; Naranjo, J. R. *Brain Res.* **1988**, *455*, 205; Hay, C. H.; Trevethick, M. A.; Wheeldon, A.; Browsers, J. S.; De Bellerche, J. S. *Neuroscience* **1997**, *78*, 843.
  20. Wilson, A. W.; Medhurst, S. J.; Dixon, C. I.; Bontoft, N. C.; Winyard, L. A.; Brackenborough, K. T.; De Alba, J.; Clarke, C. J.; Gunthorpe, M. J.; Hicks, G. A.; Bountra, C.; McQueen, D. S.; Chessell, I. P. *Eur. J. Pain* **2006**, *10*, 537.
  21. Time-dependent inhibition of CYP450s was assessed in the usual manner<sup>15</sup> except that fluorescence was generated over 30 min (rather than 10 min) and IC<sub>50</sub>s were determined after each 5 min time interval. An increase in IC<sub>50</sub> of greater than two- to threefold was considered to be significant and, depending on the baseline degree of inhibition, to potentially represent a developability risk.
  22. The overlay was generated using the software FLO (Thistlesoft, Colebrook, CT06021, USA).
  23. Searches were performed with either **1** or **3** as query molecule in combination with reduced graph,<sup>24</sup> topological pharmacophore,<sup>25</sup> or 3-point pharmacophore<sup>26</sup> fingerprints. Hits from the similarity searches were clustered using frameworks (based on molecular structure)<sup>24</sup> and annotated with simple calculated properties (e.g., molecular weight, hydrogen-bond donor and acceptor counts).
  24. Harper, G.; Bravi, G. S.; Pickett, S. D.; Hussain, J.; Green, D. V. S. *J. Chem. Inf. Comput. Sci.* **2004**, *446*, 2145.
  25. Schneider, G.; Neidhart, W.; Giller, T.; Schmid, G. *Angew. Chem., Int. Ed.* **1999**, *38*, 2894.
  26. Horvath, D. In *Cheminformatics Approaches to Virtual Screening*; Varnek, A., Tropsha, A., Eds.; Royal Society of Chemistry: Cambridge, 2008; pp 44–72.
  27. Also see WO 2008/003697A1 for additional synthetic details.
  28. <http://www.cerep.fr>.
  29. FeSSIF: Fed-state-simulated intestinal fluid. Galia, E.; Nicolaides, E.; Horter, D.; Lobenberg, R.; Reppas, C.; Dressman, J. B. *Pharm. Res.* **1998**, *15*, 698.
  30. All experiments were performed in accordance with the United Kingdom Animals (Scientific Procedures) Act, 1986 under Project Licence as well as under the review and approval of the GlaxoSmithKline Procedures Review Panel. GlaxoSmithKline safety regulations were adhered to at all times.
  31. Bennett, G. J.; Xie, Y. K. *Pain* **1988**, *50*, 355.